

# Numerical Methods for Solving Time-Dependent Quantum-Mechanical Problems with Applications

LESLIE N. SMITH,\* STUART D. AUGUSTIN, AND HERSCHEL RABITZ

*Department of Chemistry, Princeton University, Princeton, New Jersey 08544*

Received April 8, 1981; revised November 24, 1981

Two numerical techniques which can be applied to time-dependent quantum-mechanical problems are described and compared with a predictor-corrector-type method. The first method, the piecewise Magnus solution, provides an approximate solution with the exact Hamiltonian by using the first Magnus approximation over many time intervals. The second approach, the piecewise analytical solution, produces the analytical solution to an approximate Hamiltonian obtained by ignoring off-diagonal elements within each small time interval. Several illustrative model problems are reported in which the speed and accuracy of these procedures were compared with a standard Gear package. Included in these examples is the physically interesting problem of using the stimulated Raman effect to produce selectively excited molecules. Within this problem the quality of the rotating wave approximation is tested. In cases with highly oscillatory wave functions, it was found that the piecewise solution methods performed well while the Gear program was incapable of providing a reliable solution.

## I. INTRODUCTION

A broad range of physically interesting problems can be described by the time-dependent Schrödinger equation

$$i\hbar \frac{d}{dt} \Psi(t) = \mathbf{H}(t) \Psi(t). \quad (1)$$

One important application is the interaction of a molecule with an electromagnetic field [1-25]<sup>1</sup>, which includes a variety of research areas such as spectroscopy [6-11] and multiphoton adsorption [10-21]. Despite the tremendous chemical interest in understanding the interaction of radiation and matter, few accurate calculations exist [13-21]. In part, this is due to the difficulty in solving the necessary set of coupled differential equations when the solutions are highly oscillatory or at times which are large compared to the size of an oscillation.

From a mathematical point of view Eq. (1) represents a system of homogeneous,

\* Present address: Exxon Production Research Company, P.O. Box 2189, Houston, Texas 77001.

<sup>1</sup> There exists a tremendous amount of literature on the various aspects of this subject. Only a few pertinent references will be given here.

first-order, ordinary differential equation boundary-value problems, and in physical applications the dimensionality of the system is typically in the range 10–100. Difficulties associated with the large number of equations and the possible presence of highly oscillatory terms are a primary motivation for seeking specialized numerical techniques for dealing with Eq. (1). A commonly used procedure for solving systems of ODEs is based on the predictor–corrector method [26]. This approach attempts to follow the solution vector and has difficulties if the equations are stiff or if the solutions are rapidly varying. Although methods exist for handling stiff sets of equations [27], they may not be practical when the solutions are highly oscillatory. Floquet theory has been successfully applied to a radiation field problem with highly oscillatory solutions [14, 15], but this theory requires that the Hamiltonian matrix  $\mathbf{H}(t)$  be periodic. A recent work has proposed a method which can be used when there is only a single high frequency [28]. Unfortunately, many interesting physical applications do not comply with the restrictions necessary for either of these last two approaches.

In this paper, we shall describe and apply two methods which are particularly useful for problems with highly oscillatory solutions. Many details of the first technique have been previously described [30], and it has been used for calculations of collisional inelasticity [30] and radiative interactions [20, 21]. We shall show that this numerical procedure has great potential in these time-dependent studies. The second approach can be derived in part from other sources [31], but it has not been used for the solution of first-order differential equations. We illustrate all the necessary changes to adopt the procedure to solve Eq. (1).

Section II contains a description of the details of the theory for each method, and the standard Gear package which was used for comparison is briefly described. The results of illustrative examples, in which the three different methods were compared for accuracy and speed, are presented in Section III. Finally, a summarization of the results appears in Section IV.

## II. INTEGRATION TECHNIQUES

In this section, we shall present three methods for solving the time-dependent Schrödinger equation. The first, the piecewise Magnus solution, produces an approximate solution to the set of coupled first-order differential equations which arise from the expansion of the time-dependent Schrödinger equation in a basis set. The second technique, the piecewise analytic solution, yields an analytical solution to an approximate Hamiltonian. The third method, a package developed by Gear [27], directly follows the solution to the set of differential equations. The first two procedures follow the Hamiltonian while the step size of the third technique depends on the behavior of the solution.

Since there is a basic difference in how these methods obtain their solutions, there exist separate classes of problems in which one approach is superior to the others. Time-dependent problems in which there are rapid variations in the solution are very

difficult for the Gear program to deal with; thus, the piecewise Magnus solution or the piecewise analytical solution methods would be superior. When rapid-time variations exist in the Hamiltonian, then the Gear package may be best able to handle the problem. The benefits of each technique will be discussed more fully later.

An analysis of the error is included below for the two piecewise solution methods. This is important for practical applications since one would like to control the error in the solutions by varying the step sizes.

A. *The Piecewise Magnus Solution Method*

1. *Theory*

In 1954 Magnus published [32] a series solution to a set of first-order differential equations

$$\frac{d}{dt} \mathbf{Y}(t) = \mathbf{A}(t) \mathbf{Y}(t) \tag{2}$$

of the form

$$\mathbf{Y}(t) = \exp[\mathbf{\Omega}(t)] \mathbf{Y}(0), \tag{3}$$

where

$$\begin{aligned} \mathbf{\Omega}(t) = & \int_0^t \mathbf{A}(\tau) d\tau + \frac{1}{2} \int_0^t \left[ \mathbf{A}(\tau), \int_0^\tau \mathbf{A}(\sigma) d\sigma \right] d\tau \\ & + \frac{1}{4} \int_0^t \left[ \mathbf{A}(\tau), \int_0^\tau \left[ \mathbf{A}(\tau), \int_0^\sigma \mathbf{A}(\rho) d\rho \right] d\sigma \right] d\tau \\ & + \frac{1}{12} \int_0^t \left[ \left[ \mathbf{A}(\tau), \int_0^\tau \mathbf{A}(\sigma) d\sigma \right], \int_0^\tau \mathbf{A}(\sigma) d\sigma \right] d\tau + \dots \end{aligned} \tag{4}$$

This solution was independently rederived later by Pechukas and Light [33].

Pechukas and Light applied Magnus' solution to the time-dependent Schrödinger equation, illustrating the potential of the technique. Chan, Light and Lin [30] applied the piecewise Magnus solution method to a time-independent inelastic molecular-collision problem. The approach they suggest consists of two facets

(a) Divide the time-integration interval into many steps. The solution would then be given by

$$\Psi(t_n) = \prod_{i=0}^{n-1} \exp[\mathbf{\Omega}(t_{n-i}, t_{n-i-1})] \Psi(0). \tag{5}$$

There is no approximation involved in this expression.

(b) Use only the first term in the solution series given in Eq. (4). For the time-dependent Schrödinger equation we would then have

$$\Omega(t_n, t_{n-1}) = \frac{-i}{\hbar} \int_{t_{n-1}}^{t_n} \mathbf{H}(t) dt. \quad (6)$$

The use of only this first term in the series is known as the first Magnus approximation.

The magnitude of the error in this approach depends on the size of the steps, and usually the step size is reduced until the desired accuracy is achieved. Since Eq. (6) is exact when  $\mathbf{H}$  is independent of time, the approximation given in (6) is accurate when the change in the Hamiltonian is small over the time interval. Somewhat different considerations apply, however, when  $\mathbf{A}(t)$  is highly oscillatory. The terms in the Magnus series are integrals over the time step, and destructive interference may cause these integrals to decrease for larger time intervals. It may thus be advantageous to use large steps for oscillatory Hamiltonian matrices. This point will be expanded upon later.

The same technique was rederived later by Nielson and Gordon [34] who applied it to collisional studies. The method was found to be fast and accurate. A variant of this procedure was used by Walker and Preston [13] to describe a multiple photon excitation of an anharmonic oscillator. It has recently been suggested as an efficient method for treating more general radiative problems [20, 21].

A related form of the piecewise Magnus solution method is given by Askar [35] in his description of the stroboscopic method. The stroboscopic method eliminates the time dependence in the Hamiltonian within each time step while retaining the time variations between steps. This has the effect of removing the high-frequency time variations and keeping the slower systematic behavior of the solution.

## 2. Error Analysis

The error estimate of this section is obtained by examining the norm of the contribution made by the second term in the Magnus series for  $\Omega(t)$  in Eq. (4). Assuming that the time interval is small enough that  $\mathbf{H}(t)$  varies very little, we obtain the approximation for the single step absolute error in  $\Omega(t)$ ,

$$E(t_{i+1}) = \frac{(t_{i+1} - t_i)^2}{3\hbar^2} \left[ \max_{1 \leq k, l \leq N} (H_{kl}(t_{i+1})) \max_{1 \leq k, l \leq N} (H_{kl}(t_{i+1}) - H_{kl}(t_i)) \right], \quad (7)$$

where  $H_{kl}(t_i)$  is the  $(k - l)$ th element of the Hamiltonian matrix evaluated at  $t_i$ . Since the solution is related to an exponential of  $\Omega$ , this is an estimate of the norm of the relative error of the solution, provided that  $\Delta t = (t_{i+1} - t_i)$  is small enough that the noncommutativity of the matrices can be neglected. It may be noted that Eq. (7) indicates that the error is reduced whenever  $\Delta t$  is small, the norm of  $\mathbf{H}$  is small, or  $\mathbf{H}$  is nearly time independent. The next contribution to the error of  $\Omega$  can be seen from Eq. (4) to be of the order of  $(\Delta t)^3$  multiplied by the size of the triple commutators.

The starting point for obtaining Eq. (7) is an expression given by Pechukas and Light [33] for the leading term in the remainder of the Magnus series

$$E(t_{i+1}) \leq H_m H'_m (\Delta t)^3 / 3\hbar^3, \quad (8)$$

where

$$H_m = \max_{t_i \leq t \leq t_{i+1}} \|H(t)\|, \quad H'_m = \max_{t_i \leq t \leq t_{i+1}} \|H'(t)\| \quad (9)$$

and  $H'(t)$  is the derivative of the Hamiltonian. The first approximation we introduce is to evaluate the Hamiltonian at the endpoint of the time interval,  $t_{i+1}$ , rather than finding the time  $t$  over the interval in which the norm of the Hamiltonian is largest. The second approximation is

$$H'(t_{i+1}) \approx (H(t_{i+1}) - H(t_i)) / (t_{i+1} - t_i). \quad (10)$$

When one chooses the maximum matrix element of the Hamiltonian as the norm, Eq. (8) reduces to Eq. (7). Neilson and Gordon [34] used an error expression which is equivalent to Eq. (7) but gave no derivation.

In this work the value of  $E(t_i)$  was used to determine the step size for the next time interval by comparing  $E(t_i)$  with a tolerance parameter  $T$ . Arguments have been given [36] to support a formula of the form

$$\hbar^{\text{new}} = [T/E(t_i)]^{1/(n+1)} \hbar^{\text{old}}, \quad (11)$$

where  $h$  is the step size and  $n$  is the order of the approximation in an iterative process. Since one can construct an iterative process in which our solution is first order,  $n$  is one and we arrive at

$$(\Delta t)_{n+1} = (\Delta t)_i [T/E(t_i)]^{1/2} \quad (12)$$

which we subject to certain restrictions. The first condition is that the error in this last step not exceed the tolerance parameter times a chosen factor. If  $(\Delta t)_{i+1}$  was smaller than  $(\Delta t)_i$  by more than some specified factor (usually 2), then the previous step was redone with the smaller step size. Despite the extra work involved in recomputing the same step, it is important that no one step introduce a large error into the solution. The second condition on Eq. (12) was that  $(\Delta t)_{i+1}$  not exceed  $(\Delta t)_i$  by the same factor as above (although one may choose another factor if desired). This precaution was taken to keep the step size from growing too large from simply a fortuitous small error in the previous step. For more accurate calculations the factor could be made smaller than 2. These two conditions taken together provided a range of acceptable errors around the magnitude of the tolerance parameter.

The error analysis presented in this section can be improved when  $H(t)$  is highly oscillatory. In this case, cancellation effects will make the time integral of the commutator (the second term in Eq. (4)) smaller than is indicated by Eq. (7), leading

to an overestimate of the error. This destructive interference will actually cause the higher order terms of Eq. (4) to decrease as  $(\Delta t)$  is increased, and the strategy of reducing  $(\Delta t)$  to the point where  $H(t)$  varies little over the interval becomes very inefficient. Thus, for highly oscillatory Hamiltonians, it would seem advantageous to reduce the error by keeping more terms in Eq. (4) rather than by reducing the size of the time steps. An appropriate error analysis must first be developed before this approach can be implemented. However, one of the examples presented in Section III.A demonstrates that very large steps can be used with the first Magnus approximation for a highly oscillatory Hamiltonian.

### B. The Piecewise Analytical Solution Method

#### 1. Theory

The logic behind this method is based on our ability to solve an uncoupled set of differential equations. If the Hamiltonian can be transformed to a diagonal matrix, we can easily solve the problem. Since it requires as much effort to find a time-dependent transformation as it does to obtain the solution directly, we approximately diagonalize the Hamiltonian by using the transformation which diagonalizes it at the center of a small time interval and ignore the off-diagonal elements.

The method can be described as follows: The Schrödinger equation is rewritten as

$$i\hbar \frac{d}{dt} \psi(t) = \mathbf{H}(t) \psi(t) = (\mathbf{A} + \mathbf{B}f(t) + \mathbf{C}g(t) + \dots) \psi(t), \quad (13)$$

where  $\mathbf{A}$ ,  $\mathbf{B}$ , and  $\mathbf{C}$  are constant matrices and  $f(t)$  and  $g(t)$  are integrable functions of time. As a point of flexibility, one may ignore time dependencies in the Hamiltonian (e.g., high frequency terms as in the stroboscopic method [35]) which will be unimportant in the solution, but the expansion must remain Hermitian. A time interval is chosen such that the time variation in the Hamiltonian is small and the unitary matrix  $\mathbf{U}$  is obtained which diagonalizes  $\mathbf{H}$  at the center of the interval,  $t_0$ . Hence, Eq. (13) becomes

$$\begin{aligned} i\hbar \frac{d}{dt} \mathbf{U}^\dagger \psi(t) &= \mathbf{U}^\dagger \mathbf{H}(t) \mathbf{U} \mathbf{U}^\dagger \psi(t) \\ &= \mathbf{U}^\dagger (\bar{\mathbf{A}} + \mathbf{B}[f(t) - f(t_0)] + \mathbf{C}[g(t) - g(t_0)] + \dots) \mathbf{U} \mathbf{U}^\dagger \psi(t) \\ &= (\boldsymbol{\Lambda} + \mathbf{U}^\dagger \mathbf{B} \mathbf{U} \bar{f}(t) + \mathbf{U}^\dagger \mathbf{C} \mathbf{U} \bar{g}(t) + \dots) \mathbf{U}^\dagger \psi(t), \end{aligned} \quad (14)$$

where  $\bar{f}(t) = f(t) - f(t_0)$  and  $\bar{g}(t) = g(t) - g(t_0)$ ,  $\bar{\mathbf{A}}$  is equal to  $\mathbf{H}$  at  $t_0$  and  $\boldsymbol{\Lambda}$  is the resulting diagonal matrix after the transformation. Generally,  $\mathbf{U}^\dagger \mathbf{B} \mathbf{U}$  and  $\mathbf{U}^\dagger \mathbf{C} \mathbf{U}$  will not be diagonal, but it is reasonable to ignore the off-diagonal elements when they are slowly varying on the interval. Therefore, we obtain a set of uncoupled differential equations

$$i\hbar \frac{d}{dt} \mathbf{U}^\dagger \psi(t) \cong (\boldsymbol{\Lambda} + \bar{\mathbf{B}}\bar{f}(t) + \bar{\mathbf{C}}\bar{g}(t) + \dots) \mathbf{U}^\dagger \psi(t), \quad (15)$$

where  $\bar{\mathbf{B}}$  and  $\bar{\mathbf{C}}$  are the diagonal portions of  $\mathbf{U}^\dagger \mathbf{B} \mathbf{U}$  and  $\mathbf{U}^\dagger \mathbf{C} \mathbf{U}$ , respectively. Equation (15) has the analytical solution

$$\Psi(t_{i+1}) = \mathbf{U} \exp \left[ -\frac{i}{\hbar} (\mathbf{A}(t_{i+1} - t_i) + \bar{\mathbf{B}} \int_{t_i}^{t_{i+1}} \bar{f}(t) dt + \bar{\mathbf{C}} \int_{t_i}^{t_{i+1}} \bar{g}(t) dt + \dots) \right] \mathbf{U}^\dagger \Psi(t_i) \tag{16}$$

which may be generalized to include any number of functional dependencies. For simplicity in future equations, only one functional time dependence  $\bar{f}(t)$  will be retained.

A similar approach is described by Gordon [31] in order to solve the time-independent Schrödinger equation for scattering applications. Since he was dealing with a second-order equation, however, it was necessary for Gordon to approximate the potential by a linear or quadratic polynomial in order to obtain known, analytic solutions. This additional approximation is not required in the present case.

### 2. Error Analysis

Although there exist several error analyses for the piecewise analytical solution method applied to second-order differential equations [34, 36], little of this work may be carried over to the present problem. The estimate for the error used here is

$$E(t_{i+1}) = \left[ \prod_{l=1}^N \frac{3 |\sum_{k \neq l} (U^\dagger B U)_{kl} f(t_{i+1})(U^\dagger \Psi(t_{i+1}))_k|}{2 |(A_{kl} + \bar{B}_{ll} f(t_{i+1}))(U^\dagger \Psi(t_{i+1}))_l| + |\sum_{k \neq l} (U^\dagger B U)_{kl} f(t_{i+1})(U^\dagger(t_{i+1}))_l|} \right]^{1/N} \tag{17}$$

The function  $E(t_{i+1})$  is not proportional to the error but does vary directly with the error.

Equation (17) may be derived as the approximate error in the solution due to ignoring the off-diagonal elements  $(U^\dagger B U)_{ij}$ . To this end, note that the solution presented in Eq. (16) can be considered the first-order solution of the iteration scheme

$$\begin{aligned} i\hbar \frac{d}{dt} \xi_k^{(1)} &= [A_{kk} + \bar{B}_{kk} \bar{f}(t)] \xi_k^{(1)}(t) \\ i\hbar \frac{d}{dt} \xi_k^{(2)}(t) &= [A_{kk} + \bar{B}_{kk} \bar{f}(t)] \xi_k^{(2)}(t) + \sum_{l \neq k} (U^\dagger B U)_{kl} \bar{f}(t) \xi_l^{(1)}(t) \\ &\vdots \\ i\hbar \frac{d}{dt} \xi_k^{(n)}(t) &= [A_{kk} + \bar{B}_{kk} \bar{f}(t)] \xi_k^{(n)}(t) + \sum_{l \neq k} (U^\dagger B U)_{kl} \bar{f}(t) \xi_l^{(n-1)}(t), \end{aligned} \tag{18}$$

where  $\xi_k^{(1)}(t) = (\mathbf{U}^\dagger \Psi(t))_k$ . Although it is not practical to obtain the second-order solution, one may use the second-order equation to obtain an estimate of the error.

This estimate of the error (from ignoring the off-diagonal elements) can be obtained by considering the ratio of the off diagonal to the diagonal elements:

$$\left\| \frac{\sum_{k \neq l} (U^\dagger B U)_{kl} \bar{f}(t) \xi_k^{(1)}(t)}{[A_{kk} + \bar{B}_{kk} \bar{f}(t)] \xi_l^{(1)}(t)} \right\|. \tag{19}$$

This expression will improperly blow up when  $\xi_l^{(1)}(t)$  is zero for any  $k$ . In the time-independent case [36] this difficulty arose when evaluating the error as

$$\left\| \frac{\xi_l^{(2)} - \xi_l^{(1)}}{\xi_l^{(2)}} \right\| \tag{20}$$

and was avoided by taking the error in the  $l$ th element to be

$$E_l(t) = \left\| \frac{|\xi_l^{(2)} - \xi_l^{(1)}| + L_l |\xi_l^{(2)} - \xi_l^{(1)}|}{(|\xi_l^{(2)}| + L_l |\xi_l^{(2)}|)} \right\|, \tag{21}$$

where  $L_l$  is chosen such that

$$\xi_l^{(1)} \sim L_l \xi_l^{(1)}. \tag{22}$$

Here,  $L_l$  may be easily extracted from the first equation in Eq. (18) while the quantity  $|\xi_l^{(2)}(t) - \xi_l^{(1)}(t)|$  may be obtained from the first two equations in Eq. (18). If one takes the ratio in Eq. (19) as approximately the same as Eq. (20), then

$$\xi_l^{(2)}(t) - \xi_l^{(1)}(t) \sim \frac{\xi_l^{(2)}(t)}{\xi_l^{(1)}(t)} \frac{\sum_{k \neq l} (U^\dagger B U)_{kl} \bar{f}(t) \xi_k^{(1)}(t)}{[A_{kk} + \bar{B}_{kl} \bar{f}(t)]}. \tag{23}$$

Hence, we obtain

$$\begin{aligned} & |\xi_l^{(2)}(t) - \xi_l^{(1)}(t)| + L_l |\xi_l^{(2)} - \xi_l^{(1)}| \\ & \sim \left| \left( 2 \frac{\xi_l^{(2)}(t)}{\xi_l^{(1)}(t)} + 1 \right) \frac{\sum_{k \neq l} (U^\dagger B U)_{kl} \bar{f}(t) \xi_k^{(1)}(t)}{[A_{kk} + \bar{B}_{kk} \bar{f}(t)]} \right|, \end{aligned} \tag{24}$$

and Eq. (21) becomes

$$E_l(t) \sim \left\| \frac{\left| \left( 2 \frac{\xi_l^{(2)}(t)}{\xi_l^{(1)}(t)} + 1 \right) \frac{\sum_{k \neq l} (U^\dagger B U)_{kl} \bar{f}(t) \xi_k^{(1)}(t)}{[A_{kl} + \bar{B}_{ll} \bar{f}(t)]} \right|}{2 |\xi_l^{(2)}| + \left| \frac{\sum_{k \neq l} (U^\dagger B U)_{kl} \bar{f}(t) \xi_k^{(1)}(t)}{[A_{ll} + \bar{B}_{ll} \bar{f}(t)]} \right|} \right\| \tag{25}$$

where  $\xi_k^{(2)}$  was replaced by the right side of the second equation in Eq. (18). Unfortunately, it is difficult to obtain  $\xi_l^{(2)}(t)$ , so we approximate it by  $\xi_l^{(1)}(t)$ .

Equation (25) is an estimate of the relative error in the  $l$ th component of  $\mathbf{U}^\dagger \psi$



during the time interval  $t_i$  to  $t_{i+1}$ . If  $f(t)$  is expanded in a Taylor series about  $t_0$ , the midpoint of this interval,

$$f(t) \simeq f(t_0) + (\Delta t/2) f'(t_0) + (\Delta t/2)^2/2f''(t_0) + \dots,$$

it may be readily seen that  $\bar{f}$  goes to zero as the leading term (for small  $\Delta t$ ) in this series. The analysis thus predicts that the error in each component will depend on  $\Delta t$  in the same way as  $\bar{f}(t)$ . If the geometric mean of the errors in the component of  $\xi$  is taken to be the estimate of the single step relative error in the vector  $\psi$ , then Eq. (17) is obtained. The geometric mean was used because it was found to perform better than various other possible measures of the magnitude of the error.

The error estimate was used in the same manner as described in the previous error analysis Section II.A.2. Equation (12) was used to find the new step size subject to the same conditions.

### C. The Gear Integration Package

Many different algorithms have been proposed for the solution of ordinary differential equation initial-value problems. For purposes of comparing with the two methods proposed in this work, we have chosen the Gear integration package [27] as a representative of ODE solvers which are currently available. This package contains an Adams–Moulton predictor–corrector and an algorithm developed by Gear for stiff differential equations. In the examples that follow both the predictor–corrector and stiff methods were tested to find which yielded the faster, more accurate result. Since the equations are stiff only for those examples (and values of the parameters) where the Hamiltonian matrix contains highly oscillatory elements, in most cases the Adams–Moulton method was used. For brevity we shall refer to either as the Gear approach.

The important distinction between this technique and the previous two approaches is that here one must directly follow the solution. If there are many oscillations in the solution, the Gear procedure requires many small steps. The piecewise solution methods can utilize few steps and, hence, require less computational labor than this approach when each step can contain many oscillations of the solution.

## III. ILLUSTRATIVE EXAMPLES

In this section we shall compare the various techniques outlined above and discuss the speed and accuracy of each approach. The comparisons are performed by employing examples in which each procedure may be used. Results are compared with analytical solutions wherever possible. We shall illustrate cases when the piecewise analytical solution methods are clearly superior to Gear's package and vice versa.

### A. Time-Independent Hamiltonian Model

If the Hamiltonian is independent of time the analytical solution to Eq. (1) may be easily obtained. However, we can transform the problem into the interaction representation and introduce a time dependence into the problem in order to provide a non-trivial test of the methods of solution. For simplicity, we will deal with a two-state problem. A two-state time-independent Hermitian Hamiltonian may be written

$$\mathbf{H} = \begin{pmatrix} a & b \\ b^* & d \end{pmatrix} = \begin{pmatrix} a & 0 \\ 0 & d \end{pmatrix} + \begin{pmatrix} 0 & b \\ b^* & 0 \end{pmatrix} = \mathbf{H}_0 + \mathbf{V}, \quad (26)$$

where  $a$  and  $d$  are real. Introducing the transformation

$$\psi(t) = e^{-(i/\hbar)\mathbf{H}_0 t} \phi(t), \quad (27)$$

the Schrödinger equation becomes

$$i\hbar \dot{\phi}(t) = e^{(i/\hbar)\mathbf{H}_0 t} \mathbf{V} e^{-(i/\hbar)\mathbf{H}_0 t} \phi(t) = \begin{pmatrix} 0 & be^{(i/\hbar)(a-d)t} \\ b^* e^{(i/\hbar)(d-a)t} & 0 \end{pmatrix} \phi(t), \quad (28)$$

where the Hamiltonian now oscillates with time.

In the piecewise Magnus solution for this problem, we obtain from Eq. (6)

$$\Omega(t_n, t_{n-1}) = \frac{i}{\hbar} \begin{pmatrix} 0 & \frac{\hbar b}{i(a-d)} [e^{(i/\hbar)(a-d)t_n} - e^{(i/\hbar)(a-d)t_{n-1}}] \\ \frac{\hbar b^*}{i(d-a)} [e^{(i/\hbar)(d-a)t_n} - e^{(i/\hbar)(d-a)t_{n-1}}] & 0 \end{pmatrix} \quad (29)$$

on each time interval  $[t_{n-1}, t_n]$ . Exponentiation of the matrix can be done in many ways [37], but we simply transformed  $\Omega$  to a diagonal matrix, exponentiated and transformed back. In costly problems it may be useful to compare techniques for exponentiating the matrix to determine which one is most efficient [37].

For the piecewise analytical solution we expanded the Hamiltonian at the center of each time interval as

$$\mathbf{H} = \begin{pmatrix} 0 & be^{(i/\hbar)(a-d)t} \\ b^* e^{(i/\hbar)(d-a)t} & 0 \end{pmatrix} = \begin{pmatrix} 0 & be^{(i/\hbar)(a-d)t_0} \\ b^* e^{(i/\hbar)(d-a)t_0} & 0 \end{pmatrix} \\ + \begin{pmatrix} 0 & b \\ 0 & 0 \end{pmatrix} (e^{(i/\hbar)(a-d)t} - e^{(i/\hbar)(a-d)t_0}) + \begin{pmatrix} 0 & 0 \\ b^* & 0 \end{pmatrix} (e^{(i/\hbar)(d-a)t} - e^{(i/\hbar)(d-a)t_0}) \quad (30)$$

which involves two functions of time. One cannot ignore either of the functions of time, since that would lead to a non-Hermitian matrix. The first matrix on the right side of Eq. (30) is diagonalized and the transformation is applied to the other two matrices, as previously described. One can see that there is more matrix manipulation

in this method than in the piecewise Magnus solution and this approach was found to be more time consuming.

The results at  $t = 10.0$  for calculations with each of the three techniques and the initial condition

$$\psi(0) = \begin{pmatrix} 1 \\ 0 \end{pmatrix} \quad (31)$$

are presented in Tables I and II. Atomic units (a.u.) were used in this calculation (i.e.,  $\hbar = 1$ ). The results are ordered in such a way as to allow easy comparison of the

TABLE I

Comparisons of the Accuracy of Solutions for the Time-Independent Hamiltonian as a Function of  $b^a$

$b$	Execution time (s)	Number of significant figures <sup>b</sup>	Execution time (s)	Number of significant figures	Execution time (s)	Number of significant figures
1.0	0.020	2	0.035	3	0.050	4
		1		2		3
		1		4		7
2.0	0.025	3	0.050	3	0.10	4
		1		2		3
		0		3		8
3.0	0.030	2	0.075	3	0.10	4
		1		2		2
		0		5		7
5.0	0.040	2	0.080	3	0.13	3
		1		2		2
		0		2		6
10.0	0.075	2	0.15	3	0.30	4
		1		2		3
		0		3		6
20.0	0.060	1	0.25	3	0.66	4
		1		2		3
		0		3		6
30.0	0.070	1	0.37	2	1.3	4
		1		2		3
		0		1		6
100.0	0.15	2	1.2	4	2.8	5
		2		3		3
		0		2		5

<sup>a</sup> The integration period was performed from  $t = 0$  to 10 a.u. and the other parameter values are  $a = 1.1$  and  $d = 1.0$ .

<sup>b</sup> The numbers in decreasing order correspond to the Magnus, piecewise analytic, and Gear methods.

TABLE II

Comparisons of the Accuracy of Solutions in the Time-Independent Hamiltonian as a Function of  $a^a$ 

$a$	Execution time (s)	Number of significant figures <sup>b</sup>	Execution time (s)	Number of significant figures	Execution time (s)	Number of significant figures
2.0	0.030	1	0.050	1	0.10	2
		1		1		2
		1		5		8
3.0	0.030	1	0.070	1	0.10	2
		0		1		2
		1		6		7
5.0	0.030	1	0.10	1	0.50	2
		0		1		2
		0		5		8
10.0	0.030	1	0.10	1	0.70	2
		0		1		2
		0		3		8
20.0	0.030	1	0.18	1	0.85	2
		0		1		1
		0		3		8
100.0	0.030	1	0.60	1	1.6	2
		0		1		2
		0		3		7

<sup>a</sup> The integration period was performed from  $t = 0$  to 10 a.u. and the other parameter values are  $b = 1$  and  $d = 1.0$ .

<sup>b</sup> The numbers in decreasing order correspond to the Magnus, piecewise analytic, and Gear methods.

methods. The tables give the number of figures which agree with the analytical wave function  $\psi(t)$  from each of the three techniques for a given execution time. For this and all the subsequent test problems, repeated runs were performed at different tolerances, using interpolation, if necessary, to obtain data for prescribed execution times. In Table I, we kept  $a = 1.1$  and  $d = 1.0$  constant and varied  $b$ , which is real for simplicity. This has the effect of increasing the amplitude of the oscillations in the Hamiltonian and the number of oscillations in the solution. As  $b$  increases, the Gear package requires the largest increase in execution time to attain the same accuracy. In all cases the piecewise Magnus solution attains the same or better accuracy as the piecewise analytical solution method. Plots of the amplitude of the solutions indicate just over three oscillations for  $b = 1.0$ , and over 53 oscillations for  $b = 10.0$ .

In Table II, we list the results of calculations in which  $b = 1.0$  and  $d = 1.0$  were kept constant but  $a$  was varied. Increasing  $a$  has the effect of introducing oscillations into the Hamiltonian and decreasing the effective interaction between the states. The

result is that the amplitudes of each state remain near their initial values. For  $a = 10.0$ ,  $b = d = 1.0$  the probability amplitude changes by at most 0.05.

When  $a$  is large, the piecewise Magnus solution method can attain an approximate solution with few steps. This arises because the commutator term of the Magnus series can be shown to be inversely proportional to  $(a - d)^2$ . It was found for  $a = 1000.0$ ,  $b = d = 1.0$ , that the piecewise Magnus solution method yields three-figure accuracy in a single step. This is one of the cases where Eq. (7) provides an error estimate which is too conservative.

From Table II one can see that it is difficult for either of the piecewise methods to obtain accurate solutions. Here, the Gear program yields three or more figure accuracy with less execution time than either of the piecewise methods.

Several general features of these techniques are apparent from these tables. The piecewise Magnus solution and the piecewise analytical solution methods attain approximate results before the Gear approach. The Gear program can attain highly accurate solutions with less additional execution time, however, once an approximate wave function is obtained. This indicates an important factor to aid in the choice of the optimum method for a given problem. If one wishes to obtain one to three accurate figures in the wave functions, then the piecewise solution methods will be preferable. But if highly accurate wave functions (more than 4 figures) are desired, the Gear approach often will be preferable.

Another important factor in comparing techniques lies in the number of initial conditions (i.e., initial quantum states) one wishes to study. Since most of the work in the piecewise solution methods arise from the manipulation of the Hamiltonian matrix, more initial conditions may be performed with a trivial amount of additional computer time. However, the Gear program in its present form must be completely rerun. In performing the second initial condition for this problem,

$$\psi(0) = \begin{pmatrix} 0 \\ 1 \end{pmatrix} \quad (32)$$

with all the values of the constants given in Tables I and II, it was found that the piecewise solution methods required only 10% of the original execution time. There are ways in which the Gear program can be used to obtain all the initial conditions in a single run. However, it must be remembered that typical physical applications have many more coupled equations than this simple test problem. Then it will often be impractical to increase the dimensionality of the problem by combining several initial conditions in the solution vector.

### B. *Spin and Molecular Floppers*

The spin flopper problem arises when a particle with intrinsic angular momentum is subjected to a magnetic field which couples the angular momentum projection states. For a spin  $\frac{1}{2}$  system, such a field can effectively cause the spin to flop over.

Calculations [22, 23] and experiments [24] on a spin 1 system have been performed. In this case, a model of the flopper field is given by

$$\begin{aligned} &= M_r \hat{x} + M_0(t) \hat{z}, & -z_0 \leq r \leq z_0, \\ &= M_0 \hat{z}, & r > z_0, \end{aligned} \quad (33)$$

where  $M_r$  and  $M_0$  are constants and  $r$  is the distance in the  $z$  direction.  $M_0(t)$  is given by

$$M_0(t) = (v/z_0) M_0 t, \quad -t_0 \leq t \leq t_0, \quad (34)$$

where a constant particle speed  $v$  is assumed,  $2z_0$  is the length of the flopper region and  $t_0 = z_0/v$ . The particle sees a reversed field by virtue of its motion in the  $\hat{z}$  direction through the field region.

This model problem is interesting in itself and provides an opportunity to compare our results with those from an independent calculation [23]. The Schrödinger equation for this problem is given by [23],

$$i \frac{d}{dt} \begin{pmatrix} \phi_x \\ \phi_y \\ \phi_z \end{pmatrix} = \begin{pmatrix} 0 & i(\gamma_v/z_0) M_0 t & 0 \\ -i(\gamma_v/z_0) M_0 t & 0 & i\gamma M_r \\ 0 & -i\gamma M_r & 0 \end{pmatrix} \begin{pmatrix} \phi_x \\ \phi_y \\ \phi_z \end{pmatrix}, \quad (35)$$

where

$$\begin{pmatrix} \phi_x(-t_0) \\ \phi_y(-t_0) \\ \phi_z(-t_0) \end{pmatrix} = \begin{pmatrix} 0 \\ 0 \\ 1 \end{pmatrix}, \quad (36)$$

$\gamma$  is a constant which arises from the magnetic dipole moment, and  $x, y, z$  are the Cartesian components of the spin vector.

The results of several sets of calculations on this problem are presented in Table III. In these calculations  $\gamma = 1.4$  MHz/G,  $z_0 = 3.75$  cm,  $M_0 = 2.5$  G, and  $M_r = -\frac{1}{2} M_0$ . Since the length of the flopper region  $2z_0$  was constant,  $t_0$  changed as the speed  $v$  was varied in the calculation. For a velocity of  $10^6$  cm/s we have  $t_0 = 3.75 \times 10^{-6}$  s. The results illustrated in Table III support the same conclusion as indicated in the time-independent problem. At high velocities where there is very little change in the wave functions, the Gear package was superior. At slower velocities the piecewise solution methods are superior. In general, the piecewise solution methods yielded 1–3 figure accuracy in the wave function at lower execution time than the Gear routine, but the Gear package converged on highly accurate results more quickly than the piecewise solution methods.

Only one initial condition (Eq. (36)) was used in the calculations of Table III. This represents the worst condition for comparison since the piecewise solution methods

TABLE III

Execution Times and Accuracy for a Spin 1 Particle in a Flopper Field with Several Different Velocities

$V$ (cm/sec)	Execution time (s)	Number of significant figures <sup>a</sup>	Execution time (s)	Number of significant figures	Execution time (s)	Number of significant figures
$5.0 \times 10^6$	0.020	1	0.025	2	0.030	2
		1		1		2
		0		2		4
$1.0 \times 10^6$	0.025	1	0.035	2	0.050	2
		1		2		2
		1		2		4
$5.0 \times 10^5$	0.030	1	0.050	2	0.100	3
		1		1		2
		0		1		5
$1.0 \times 10^5$	0.050	1	0.100	2	0.300	3
		1		1		2
		0		0		3
$5.0 \times 10^4$	0.100	1	0.300	2	0.600	3
		1		2		2
		0		0		4
$1.0 \times 10^4$	0.600	1	1.0	3	4.0	5
		1		2		4
		0		0		3

<sup>a</sup> The numbers in decreasing order correspond to the Magnus, piecewise analytic, and Gear methods.

can handle the additional initial conditions with only a slight increase in execution time. For this problem three independent initial conditions may be performed with the piecewise solution methods for a one-fourth increase over the execution time while the Gear method requires three times longer to do the one calculation.

We also treated the related problem of a diatomic rigid rotor in a flopper-type magnetic field. Since many different rotational states are accessible, this is a more versatile and general test problem. Here the time-dependent Hamiltonian is

$$H(t) = (1/2I) \mathbf{j} \cdot \mathbf{j} - \mu \mathbf{M}(t) \cdot \mathbf{j}. \quad (37)$$

Expanding the wave function in terms of a molecular basis set

$$\psi_j(t) = \sum_{m=-j}^j a_m^j(t) |jm\rangle \quad (38)$$

leads to the coupled differential equations

$$i\hbar \frac{da_m^j(t)}{dt} = \sum_{m'=-j}^j \langle jm | \frac{1}{2I} \mathbf{j} \cdot \mathbf{j} - \mu \mathbf{M}(t) \cdot \mathbf{j} | jm' \rangle a_{m'}^j(t), \quad -j \leq m \leq j. \quad (39)$$

Using  $\mu = \gamma\hbar$  and explicitly evaluating the matrix elements, this set of equations becomes

$$i \frac{da_m^j(t)}{dt} = \sum_{m'=-j}^j \left[ \delta_{mm'} \left\{ B_0 j(j+1) + \frac{\gamma v}{z_0} M_0 t m \right\} + \delta_{mm'+1} \frac{\gamma M_r}{2} \sqrt{j(j+1) - m(m-1)} + \delta_{mm'-1} \frac{\gamma M_r}{2} \sqrt{j(j+1) - m(m+1)} \right] a_{m'}^j(t), \quad -j \leq m \leq j, \quad (40)$$

where the time dependence of the magnetic field was taken to be the same as in Eq. (34).

As Eq. (40) stands, it can be solved by the piecewise solution methods but it cannot be solved with Gear's program. This latter difficulty arises since the rotational constant  $B_0$  is typically on the order of  $10^{10}$  Hz and this introduces a highly oscillating part into the wave function. By going into an interaction representation, one may transform all or part of this oscillating function out of the solution. We can introduce an added degree of freedom in the test problem by writing  $B_0 j(j+1)$  as  $Cj(j+1) + (B_0 - C)j(j+1)$  and transforming the  $(B_0 - C)j(j+1)$  term from the Hamiltonian into the wave function. One may then compare the three techniques over the range of problems in which the Gear program goes from being efficient to being incapable of yielding a reasonable solution. We will denote the constant value which remains in each diagonal element of the Hamiltonian as  $Cj(j+1)$ .

As before, the constants in Eq. (40) were taken to be  $\gamma = 1.4$  MHz/G,  $z_0 = 3.75$  cm,  $M_r = -\frac{1}{2}M_0$ ,  $B_0 = 10^{10}$  Hz,  $v = 10^6$  cm/s, and  $t_0 = 3.75 \times 10^{-6}$  s. Setting  $j = 1$  produces a three-dimensional problem similar to the spin problem presented earlier. Table IV presents the results of calculations in which  $C$  and  $M_0$  were varied in the  $j = 1$  case. This table clearly illustrates the regions where the Gear method is inappropriate. As the magnitude of  $C$  increases, the piecewise methods are hardly affected while there is a drastic effect on the Gear solution. At a value of  $C = 10^8$  Hz one can obtain highly accurate solutions from the piecewise methods before any solution can be obtained from the Gear program. The ability of the piecewise methods to obtain the correct solution regardless of the magnitude of  $C$  indicates one of the benefits of these approaches. They "recognize" any analyticity in a problem and automatically extract it without an increase in the execution time.

To amplify the differences between the methods, calculations were performed with  $j = 4$  and this gave rise to a nine-state problem. The constants were the same as before except that  $M_0$  was held fixed at 2.5 G. Table V presents the results of



TABLE IV  
 Execution Time and Accuracy for the  $j = 1$  Molecule in a Flopper Field  
 with Several Values of  $M_0$  and  $C$

$M_0$ (G)	$C \times 10^{-7}$ (Hz)	Execution time (s)	Number of significant figures <sup>a</sup>	Execution time (s)	Number of significant figures	Execution time (s)	Number of significant figures
2.5	0.0	0.035	1	0.050	2	0.100	3
			0		1		2
			0		1		4
2.5	0.1	0.050	1	0.100	3	0.250	4
			1		2		3
			1		3		5
2.5	1.0	0.100	3	0.250	4	1.0	5
			2		3		4
			0		1		4
2.5	10.0	0.250	4	1.0	5	2.0	6
			3		4		5
			0		0		0
5.0	0.0	0.035	1	0.050	1	0.100	2
			0		1		2
			0		0		3
5.0	0.1	0.050	1	0.100	2	0.250	3
			1		2		2
			0		2		4
5.0	1.0	0.100	2	0.250	3	1.0	4
			1		2		3
			0		1		4
5.0	10.0	0.250	3	1.0	4	2.0	5
			2		3		4
			0		0		0

<sup>a</sup> The numbers in decreasing order correspond to the Magnus, piecewise analytic, and Gear methods.

calculations for this  $j = 4$  problem with variations in the value of  $C$  and either one or nine orthogonal initial conditions. The one initial condition case is  $a_m^j = \delta_{0m}$ ,  $-4 \leq m \leq 4$ , and the nine initial conditions are  $a_m^j = \delta_{m'm}$ ,  $-4 \leq m, m' \leq 4$ . This table exemplifies the benefit derived from the ability of the piecewise solution methods to handle any number of initial conditions with ease. In many of the cases in which Gear's method is faster for only one initial condition, the piecewise solution methods become superior when the nine orthogonal initial conditions given above are desired.

Figure 1 contains a plot of the probability for the  $m$  states from 0 to 4, with  $\psi$  initially one for  $m = 0$  and zero for all of the other values of  $m$ . Only the positive  $m$

TABLE V

Execution Times and Accuracy for a ( $j = 4$ ) Molecule in a Flopper Field with Several Values of  $C$  and Two Different Numbers of Initial Conditions

No. of initial conditions	$C \times 10^{-7}$ (Hz)	Execution time (s)	Number of significant figures <sup>a</sup>	Execution time (s)	Number of significant figures	Execution time (s)	Number of significant figures
1	0.0	0.35	1	0.50	1	0.75	2
			0		0		1
			1		3		4
1	0.1	0.50	1	1.0	2	2.0	3
			0		1		2
			0		2		5
1	1.0	1.0	2	7.0	4	11.0	4
			1		3		3
			0		1		3
1	10.0	7.0	4	11.0	4	20.0	5
			3		3		4
			0		0		0
9	0.0	0.75	1	2.0	2	7.0	3
			0		1		2
			0		0		4
9	0.1	2.0	2	7.0	3	16.0	4
			1		2		3
			0		1		4
9	1.0	7.0	4	25.0	5	60.0	5
			2		3		4
			0		0		1
9	10.0	25.0	5	60.0	5	200.0	6
			3		4		5
			0		0		0

<sup>a</sup> The numbers in decreasing order correspond to the Magnus, piecewise analytic, and Gear methods.

states are included in this figure since the negative  $m$  states have the identical probability amplitudes as their positive counterparts. Many oscillations exist in the probability of each  $m$  state and the phase of the wave function introduces even more variations for these methods to follow.

### C. Stimulated Resonance Raman Pumping

The stimulated resonance Raman pumping of vibrational states, which is described in detail elsewhere [25], was chosen as a problem of current interest in which the

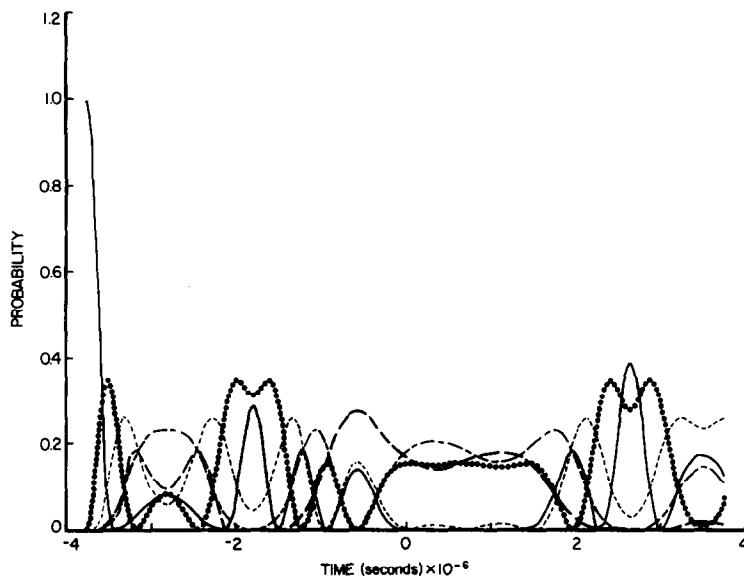


FIG. 1. Probability of the  $m$  states for a  $j=4$  molecule entering a flopper magnetic field with the initial condition being unit probability for state  $m=0$ .  $m=0$ ; —;  $m=1$ , ···;  $m=2$ , - - -;  $m=3$ , - · - ·;  $m=4$ , - - - -.

methods discussed in this work can be applied. For completeness, we present a brief description of the problem and set up the appropriate equations.

In the stimulated resonance Raman effect two lasers are employed and the intermediate state is a real excited electronic state of the molecule. Considerable intensity enhancement can be achieved in this fashion. This situation is shown in Fig. 2 with specific vibration-rotation levels drawn in.

In an experimental arrangement it may be desirable that the lasers are not in exact resonance with any of the states within the excited electronic manifold. This may help limit any difficulties due to excessive fluorescence to neighboring states in the ground manifold.

The Hamiltonian for this problem is

$$H(\mathbf{R}, t) = H_0(\mathbf{R}) - \boldsymbol{\mu}(\mathbf{R}) \cdot (\mathbf{E}_a(t) + \mathbf{E}_r(t)), \quad (41)$$

where  $H_0(\mathbf{R})$  is the Hamiltonian of the unperturbed molecule,  $\mathbf{R}$  represents all internal coordinates,  $\boldsymbol{\mu}(\mathbf{R})$  is the electric dipole-moment operator,  $\mathbf{E}_a(t)$  is the time-dependent electric field from the first laser and  $\mathbf{E}_r(t)$  is the time-dependent electric field arising from the second laser. The total wave function can be expanded as

$$\psi(\vec{R}, t) = \sum_{\substack{nv \\ jm}} C_{vjm}^n(t) e^{-i\epsilon_{vjm}^n t/\hbar} |nvjm\rangle, \quad (42)$$

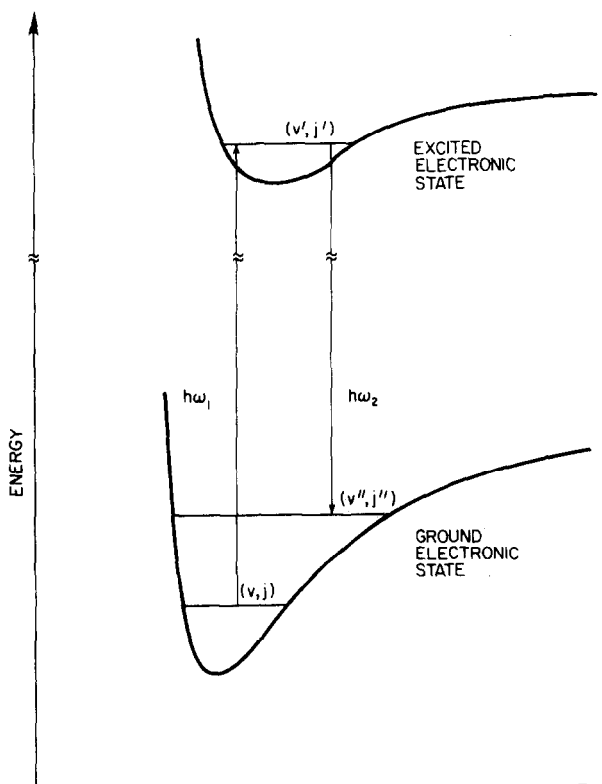


FIG. 2. Schematic representation of the stimulated resonance Raman process with two lasers of frequency  $\omega_1$  and  $\omega_2$ . Specific resonant vibration-rotation levels are shown.

where  $C_{vjm}^n(t)$  is the time-dependent amplitude for the state with the electronic, vibrational, rotational, and projection quantum numbers  $n$ ,  $v$ ,  $j$ , and  $m$ , respectively. Also,  $\epsilon_{vj}^n$  and  $|nvjm\rangle$  are the eigenvalues and eigenstates, respectively, of  $H_0(\mathbf{R})$ .

Substituting Eq. (42) into the time-dependent Schrödinger equation leads to the usual set of couple differential equations

$$i\hbar \frac{dC_{vjm}^n(t)}{dt} = \sum_{\substack{n'v' \\ j'm'}} \langle nvjm | \boldsymbol{\mu}(\mathbf{R}) \cdot (\mathbf{E}_a(t) + \mathbf{E}_r(t) | n'v'j'm' \rangle C_{v'j'm'}^{n'}(t) \\ \times \exp[i(\epsilon_{vj}^n - \epsilon_{v'j'}^{n'})t/\hbar]. \quad (43)$$

By taking the electric fields to be linearly polarized and using the Frank-Condon approximation, one may show

$$\begin{aligned}
 \langle nvjm | \boldsymbol{\mu} \cdot \mathbf{E}_a(t) | n'v'j'm' \rangle &= \langle nv | n'v' \rangle \mu^{nn'} E_a(t) \sqrt{4\pi/3} \\
 &\times \sum_{\lambda=-1}^1 Y_1^\lambda(\theta_a, \phi_a) (-1)^{m+\lambda} \sqrt{(2j+1)(2j'+1)} \\
 &\times \begin{pmatrix} j & 1 & j' \\ 0 & 0 & 0 \end{pmatrix} \begin{pmatrix} j & 1 & j' \\ m & \lambda & -m' \end{pmatrix}, \quad (44)
 \end{aligned}$$

where  $\langle nv | n'v' \rangle$  is a Franck–Condon factor,  $\mu^{nn'}$  is the electric moment between states  $n$  and  $n'$ ,  $E_a(t)$  is the time-dependent magnitude of the electric field,  $\theta_a$  and  $\phi_a$  specify the angle between the electric field and the space-fixed  $z$  axis, the  $Y$ 's are spherical harmonics, and  $\begin{pmatrix} \cdot & \cdot & \cdot \\ \cdot & \cdot & \cdot \end{pmatrix}$  is a  $3-j$  symbol. A similar expression may be written for the electric field of the second laser,  $E_r(t)$ .

We have some freedom in how we choose the space-fixed  $z$  axis and the angles of polarization of the electric fields. There is no loss of generality in choosing  $\theta_a = \phi_a = 0$  and  $\phi_r = 0$  and retaining  $\theta_r$  as the angle between the polarization of the two fields. The space-fixed  $z$  axis is chosen along the direction of  $\mathbf{E}_a(t)$ . Since  $\theta_a$  equals zero, Eq. (44) dictates that  $\Delta m = 0$  for all transitions due to the presence of the first laser.

For the time-dependent electric field strengths, we have taken

$$\begin{aligned}
 E_a(t) &= \sqrt{8\pi I_a/c} \cos(\omega_a t) \exp[-(t^2 \ln 2)/2\Delta_{1/2}^2] \\
 E_r(t) &= \sqrt{8\pi I_r/c} \cos(\omega_r t) \exp[-(t^2 \ln 2)/2\Delta_{1/2}^2], \quad (45)
 \end{aligned}$$

where  $I_a$  and  $\omega_a$  represent the intensity and frequency, respectively, of the first laser and, similarly, for  $I_r$  and  $\omega_r$  associated with the second laser. The constant  $c$  is the speed of light and  $\Delta_{1/2}$  is the full width at half maximum, which is assumed to be the same for both lasers. The two values of  $\Delta_{1/2}$  which were employed in these calculations are

$$\begin{aligned}
 \Delta_{1/2} &= 1.47 \times 10^{-11} \text{ s} \quad (\text{short pulse}) \\
 &= 7.36 \times 10^{-9} \text{ s} \quad (\text{long pulse}). \quad (46)
 \end{aligned}$$

The energy differences  $\varepsilon_{vj}^n - \varepsilon_{v'j'}^{n'}$  needed in Eq. (43) were obtained from Herzberg [38] using the  $I_2$  molecule as a model case. Between the two electronic states  $X' \Sigma_g^+$  and  $B^3\Pi_{0u}^+$ , the electronic transition moment,  $\mu^{s,e}$ , has been measured [39] as

$$\mu^{e,s} = 1.62R_c - 3.51, \quad 2.8 \text{ \AA} \leq R_c \leq 3.1 \text{ \AA} \quad (47)$$

which yields an average value of 1.27 debyes.

We choose  $\omega_a$  such that the states from  $n = g, v = 0, j = 5$  to  $n = e, v = 0, j = 6$  are in resonance. This corresponds to a value for  $\omega_a$  of  $2.93819 \times 10^{15} \text{ sec}^{-1}$  (i.e.,  $\lambda_a = 6410 \text{ \AA}$ ). Similarly,  $\omega_r$  is picked such that the states from  $n = e, v = 0, j = 6$  to  $n = g, v = 5, j = 5$  are in resonance. This requires  $\omega_r$  to be  $2.778843 \times 10^{15} \text{ s}^{-1}$  (i.e.,  $\lambda_r = 6778.55 \text{ \AA}$ ). One may evaluate the Frank–Condon overlap integrals between

these states by using uniform semiclassical Airy wave functions<sup>2</sup>. The values of the pertinent overlap integrals are

$$\langle e0|g0\rangle = 1.12 \times 10^{-4}, \quad \langle e0|g5\rangle = 1.927 \times 10^{-2}. \quad (48)$$

The values for all of the fundamental constants were obtained from Cohen and Taylor [40].

In the calculation, if one includes only the three molecular states,  $(g, 0, 5)$ ,  $(e, 0, 6)$ , and  $(g, 5, 5)$ , then the  $m$  degeneracy produces a 35-state problem. Even though previous work approximated the problem by ignoring the  $m$  dependence, we felt some new information might be gained by including the  $m$  states and examining the effect of the polarization angle on the stimulated resonance Raman process.

The time dependence of the Hamiltonian can be obtained from Eqs. (43) and (45). The functional time dependencies are of the form

$$\frac{1}{2} \{1 + \exp[\pm(5.557686 \times 10^{15})it]\} \exp[-(1.6 \times 10^{21})t^2], \quad (49)$$

where the value of  $\Delta_{1/2}$  corresponding to the short pulse was used.

As the problem stands, the Gear method cannot solve it due to the high frequency oscillations. In order to alleviate this difficulty, the rotating wave approximation is usually invoked. This involves ignoring the highly oscillatory terms in the Hamiltonian. The piecewise Magnus and the piecewise analytical solution methods, however, can handle the problem without the rotating wave approximation. This provides a test of this common approximation, in addition to indicating a clear benefit of the piecewise methods. Since all previous examples indicated that the piecewise Magnus solution was faster than the piecewise analytical solution method, especially when more than one time dependence of the Hamiltonian was present, only the piecewise Magnus solution technique was employed in the calculations on this model problem. Performing the calculation,<sup>3</sup> one finds that the rotating wave approximation is excellent in this case; wave functions obtained with and without the rotating wave approximation showed agreement in all eight significant figures which we examined.

Therefore, we invoked the rotating wave approximation. Unfortunately, the only function of time remaining in the Hamiltonian is the  $e^{-1.6 \times 10^{21}t^2}$  term and the piecewise Magnus solution method trivially (in one step) provides the analytical solution to this problem. Hence, the two procedures cannot be usefully compared here, but the problem will be changed to provide a reasonable comparison. Before introducing these changes below we first report some interesting results of this analytical calculation. Table VI contains the transition probabilities at various angles  $\theta_r$  between the laser polarization at two sets of values for  $\Delta_{1/2}$ ,  $I_a$ , and  $I_r$ . Here,  $P_{06}^e$  represents the probability amplitude after the pulse for finding the molecule in the

<sup>2</sup> The values of the overlap integrals used were obtained from [25].

<sup>3</sup> In order to evaluate some of the definite integrals, it was necessary to use an asymptotic expansion of the error function,  $\text{erf}(x + iy)$ .

TABLE VI  
Stimulated Resonance Raman Pumping Transition Probabilities for  
Various Laser Polarization Angles  $\theta_0$

$\Delta_{1/2}$	$1.47 \times 10^{-11}$ s	$7.36 \times 10^{-9}$ s		
$I_a$	$1.0 \times 10^{-11}$ W/cm <sup>2</sup>	$1.0 \times 10^9$ W/cm <sup>2</sup>		
$I_r$	$6.7 \times 10^9$ W/cm <sup>2</sup>	$1.5 \times 10^4$ W/cm <sup>2</sup>		
$\theta$ (deg)	$P_{06}^e$	$P_{55}^g$	$P_{06}^e$	$P_{55}^g$
0	$1.52 \times 10^{-4}$	$1.68 \times 10^{-3}$	0.460	0.364
30	$8.13 \times 10^{-4}$	$1.75 \times 10^{-3}$	0.530	0.251
45	$1.83 \times 10^{-3}$	$1.51 \times 10^{-3}$	0.544	0.196
60	$3.17 \times 10^{-3}$	$1.01 \times 10^{-3}$	0.511	0.207
90	$4.80 \times 10^{-3}$	$2.81 \times 10^{-4}$	0.440	0.290

state  $n = e$ ,  $v = 0$ ,  $j = 6$ , summed over the final  $m$  states. A similar definition holds for  $P_{55}^g$ . For the two sets of conditions given here DePristo *et al.* [25] reported  $P_{06}^e = P_{55}^g = 5.1 \times 10^{-4}$  and 0.49, respectively, with no angular resolution of the probabilities. The equality does not appear to hold and the first value reported earlier is a factor of 2 or 3 smaller than the results obtained here. The larger magnitude observed here is encouraging since it indicates that the stimulated resonance Raman process is more likely to be observed experimentally. It is noteworthy that the stimulated Raman process appears to be most efficient at  $\theta = 0^\circ$  in both sets of conditions.

Comparisons between the Gear and the piecewise Magnus solution methods may be performed for the stimulated resonance Raman problem by including some near resonant molecular states which are coupled in by Eq. (48). A calculation was performed including the molecular states  $(g, 0, 5)$ ,  $(e, 0, 4)$ ,  $(e, 0, 6)$ ,  $(g, 5, 3)$ ,  $(g, 5, 5)$ , and  $(g, 5, 7)$  and their corresponding  $m$  values. This results in a 66 state problem. To simplify the problem, we first examined the case with  $\theta_r = 0^\circ$ , where  $\Delta_m$  must be zero in all transitions. This uncouples the problem down to four 6-state ( $m = 0, 1, 2, 3$ ), one 5-state ( $m = 4$ ), and one 4-state ( $m = 5$ ) problem with a tremendous savings of computer time. From symmetry considerations it is clear that one would obtain the same probability amplitudes for negative  $m$  states as from positive  $m$  states, so it is not necessary to repeat the calculations for the negative  $m$  states. We impose the rotating wave approximation since the quality of the approximation has been shown to be high.

Under the short-pulse condition and any given  $m$  value, both procedures yielded two significant figures in the wave function at an execution time of about 0.06 s. At execution times on the order of 0.20 s, Gear's program provided six figures while the piecewise Magnus solution method only gave three figures. With the long-pulse conditions<sup>3</sup> the piecewise Magnus solution technique proved superior. The piecewise Magnus solution method yielded three significant figures for any one value of  $m$  with

TABLE VII

Stimulated Resonance Raman Pumping Transition Probabilities to Resonant and Near-Resonant Molecular States for Short and Long Laser Pulses

$A_{1/2}$	$1.47 \times 10^{-11}$ s	$7.36 \times 10^{-9}$ s
$I_a$	$1.0 \times 10^{11}$ W/cm <sup>2</sup>	$1.0 \times 10^9$ W/cm <sup>2</sup>
$I_r$	$6.7 \times 10^9$ W/cm <sup>2</sup>	$1.5 \times 10^4$ W/cm <sup>2</sup>
$P_{05}^g$	0.9983	0.175
$P_{04}^e$	$4.50 \times 10^{-5}$	$\sim 3 \times 10^{-10}$
$P_{06}^e$	$1.33 \times 10^{-4}$	0.461
$P_{33}^g$	$6.02 \times 10^{-5}$	$\sim 8 \times 10^{-18}$
$P_{35}^g$	$1.43 \times 10^{-3}$	0.364
$P_{37}^g$	$1.52 \times 10^{-5}$	$\sim 3 \times 10^{-10}$

execution times as low as 0.06 s while the Gear program did not provide even one significant figure until about 0.3 s and gave three-figure accuracy at 6.0 s.

The results from these calculations are listed in Table VII. Under the short-pulse conditions, one can see that the final stimulated resonance Raman product,  $P_{35}^g$  is an order of magnitude larger than the probability of the intermediate state  $P_{06}^e$ , and nearly two orders of magnitude larger than the probabilities of the near resonant states. With the long-pulse conditions,  $P_{05}^g$ ,  $P_{06}^e$ , and  $P_{35}^g$  are within an order of magnitude and the probabilities of the near-resonant states approach zero. Here, the stimulated resonance Raman pumping works very well as the population of the vibrationally excited states,  $P_{35}^g$ , is several orders of magnitude greater than the population of any nearby states. A note of caution is necessary, however, since

probabilities may be obtained but we feel that the order of magnitude estimates given above will still be valid.

An interesting feature of these results is the dramatic decrease in the probability of the near-resonant states in the long-pulse conditions compared with the short-pulse results. In part, this may be due to the smaller amount of power broadening associated with the lower intensity. There is also an increase in the resonant states' probability in going from the short pulse to the long-pulse conditions. These results indicate that the one way to effect stimulated resonance Raman pumping experimentally would be with the long-pulse conditions if resonance between the lasers' frequencies and the molecular states can be obtained.

By comparing the  $\theta = 0^\circ$  row of Table VI with Table VII one may see the effect of including additional states in the calculations. The error from neglect of states appears to be small, even under the short-pulse conditions.



## IV. CONCLUDING REMARKS

We have described and tested two numerical methods which can be applied to time-dependent quantum-mechanical problems. The methods were applied to a variety of test cases where there were several parameter variations within each problem, and the results were compared with a standard Gear package program for speed and accuracy. Stimulated resonance Raman pumping was described as a special physically relevant problem and transition probabilities were reported for a specific model.

The following conclusions can be made concerning the two piecewise approaches:

(a) The piecewise methods provide a low-order accuracy wave function (1–3 significant figures) with little execution time. In all the problems studied, an acceptable degree of accuracy was present with these techniques even when only a few large steps are used in the calculation.

(b) Convergence to a highly accurate wave function (4–8 significant figures) is usually slower than with the Gear procedure. Exceptions arise here when there are so many oscillations in the solutions that the Gear method cannot handle the problem.

(c) In problems where several initial conditions are desired, the piecewise solution methods have an advantage over Gear's program, although the latter program could, in principle, be modified to reuse repeated operations.

(d) If the Hamiltonian contains many oscillations but the solutions do not, Gear's method has an advantage. There are exceptions to this rule (for the piecewise Magnus solution approach which are described in the text).

(e) If the solutions contain many oscillations, the piecewise solution methods have the advantage.

(f) If the Hamiltonian differs only slightly from one which can be solved analytically, such as encountered in testing the rotating wave approximation, the piecewise solution techniques possess an advantage.

(g) The piecewise Magnus solution procedure proved to be faster than the piecewise analytical solution method. This appears to be due to the additional matrix manipulations required by the piecewise analytical solution method. An equivalent number of matrix manipulations between the piecewise methods can be achieved when only the constant matrix  $\mathbf{A}$  is retained in the piecewise analytical approach.

This list provides broad guidelines for choosing the appropriate method for solving quantum-mechanical time-dependent problems. Although in many cases no clear choice of methods will be possible, the observations presented here will facilitate the decision.

## ACKNOWLEDGMENTS

The authors acknowledge support for this work from the Air Force Office of Scientific Research and the Office of Naval Research.

## REFERENCES

1. C. B. MOORE, Ed., "Chemical and Biochemical Applications of Lasers," Vols. I-IV, Academic Press, New York, 1977.
2. K. SAUER, *Annu. Rev. Phys. Chem.* **30** (1979), 155.
3. J. T. KNUDSON AND E. M. EYRING, *Annu. Rev. Phys. Chem.* **25** (1974), 225.
4. S. J. ARNOLD AND H. RAJESKA, *Appl. Opt.* **12** (1973), 169.
5. J. L. KINSEY, *Annu. Rev. Phys. Chem.* **28** (1977), 349.
6. J. I. STEINFELD, "Molecules and Radiation: An Introduction to Modern Molecular Spectroscopy," MIT Press, Cambridge, Mass. 1978.
7. E. B. WILSON, *Annu. Rev. Phys. Chem.* **30** (1979), 1.
8. I. N. LEVINE, "Molecular Spectroscopy," Wiley, New York, 1975.
9. J. I. STEINFELD AND P. L. HOUSTON, "Laser and Coherence Spectroscopy" Plenum, New York, 1978.
10. P. A. SCHULZ, A. S. SUDBO, D. J. KRAJNOWICH, H. S. KWOK, Y. R. SHEN, AND Y. T. LEE, *Annu. Rev. Phys. Chem.* **30** (1979), 379.
11. R. V. AMBARTZUMIAN AND V. S. LETOKHOV, in "Chemical and Biochemical Applications of Lasers," (C. B. Moore, Ed.), Vol. III, Academic Press, New York, 1977.
12. W. M. GELBART, *Annu. Rev. Phys. Chem.* **28** (1977), 323.
13. R. B. WALKER AND R. K. PRESTON, *J. Chem. Phys.* **67** (1977), 2017.
14. S. LEASURE AND R. E. WYATT, *Chem. Phys. Lett.* **61** (1979), 625.
15. S. LEASURE AND R. E. WYATT, *Opt. Eng.* **19** (1980), 46.
16. D. W. NOID, C. BOTTCHEER, AND M. L. KOSZYKOWSKI, to appear.
17. J. H. EBERLY, B. W. SHORE, Z. BIALYNICKA-BIRULA, AND I. BIALYNICKA-BIRULA, *Phys. Rev. A* **16** (1977), 2038.
18. Z. BIALYNICKA-BIRULA, I. BIALYNICKA-BIRULA, J. H. EBERLY, AND B. W. SHORE, *Phys. Rev. A* **16** (1977), 2048.
19. R. J. COOK AND B. W. SHORE, *Phys. Rev. A* **20** (1979), 529.
20. I. SCHEK, M. L. SAGE, AND J. JORTNER, *Chem. Phys. Lett.* **63** (1979), 230.
21. S. C. LEASURE, K. F. MILFIELD, AND R. E. WYATT, *J. Chem. Phys.* **74** (1981), 6197.
22. C. R. WILLIS AND R. H. PICARD, *Phys. Rev. A* **9** (1974), 1343.
23. B. C. SANCTUARY, *Phys. Rev. A* **20** (1979), 1169.
24. (a) R. D. HIGHT, R. T. ROBISCOE, AND W. R. THORSON, *Phys. Rev. A* **15** (1977), 1079; (b) R. D. HIGHT AND R. T. ROBISCOE, *ibid.* **17** (1978), 561.
25. A. E. DEPRISTO, H. RABITZ, AND R. B. MILES, to appear.
26. M. ABRAMOWITZ AND I. A. STEGUN, "Handbook of Mathematical Functions with Formulas, Graphs, and Mathematical Tables," National Bureau of Standards, Washington, D.C., 1964.
27. C. W. GEAR, *Commun. ACM* **14** (1971), 176, 185; A. C. HINDMARSH, "Gear: Ordinary Differential Equation System Solver," UCID-30001, Rev. 3, Lawrence Livermore Laboratory, Livermore, California, 1974.
28. L. R. PETZOLD, *SIAM J. Numer. Anal.* **18** (1981), 455.
29. D. R. DION AND J. O. HIRSCHFELDER, *Advan. Chem. Phys.* **35** (1976), 265.
30. S. CHAN, J. C. LIGHT, AND J. LIN, *J. Chem. Phys.* **49** (1968), 86.
31. R. G. GORDON, *J. Chem. Phys.* **51** (1969), 14; in "Methods of Computational Physics" (B. Alder, S. Fernbach, and M. Rotenberg, Eds.), Vol. 10, Academic Press, New York, 1971.
32. W. Magnus, *Commun. Pure Appl. Math.* **7** (1954), 649.
33. P. PECHUKAS AND J. C. LIGHT, *J. Chem. Phys.* **44** (1966), 3897.
34. W. B. NEILSEN AND R. G. GORDON, *J. Chem. Phys.* **58** (1973), 4131.
35. A. ASKAR, *Phys. Rev. A* **10** (1974), 2395.
36. MITCHELL D. SMOOKE, Ph.D. Thesis, Harvard University, July 1978.
37. C. MOLER AND C. VAN LOAN, *SIAM Rev.* **20** (1978), 801.
38. G. HERZBERG, "Spectra of Diatomic Molecules," Van Nostrand-Reinhold, Princeton, N. J., 1950.
39. J. B. KOFFEND, R. BACIS, AND R. W. FIELD, *J. Chem. Phys.* **70** (1979), 2366.
40. E. R. COHEN AND B. N. TAYLOR, *J. Phys. Chem. Ref. Data* **2** (1973), 663.